RECENT RESEARCH ON GROUND MOTION DIRECTIONALITY IN STRIKE-SLIP EARTHQUAKES

Eduardo Miranda and Nathan Girmay

Department of Civil and Environmental Engineering
Stanford University

Abstract

Horizontal spectral response at a site can change considerably with orientation, in what is referred to as directionality. This paper summarizes recent and ongoing studies on ground motion directionality in strike-slip earthquakes. Ground motions from strike-slip earthquakes exhibit systematic directional patterns, with the maximum spectral response occurring near the transverse orientation. Ground motions from physics-based simulations of strike-slip earthquakes are found to exhibit directionality characteristics consistent with recorded motions, although they tend to have greater polarization at shorter periods, presumably due to smaller wave scattering than the one occurring in real earthquake ground motions. Lastly, new approaches to quantifying component-to-component variability of response spectral ordinates are introduced, and it is shown that this source of variability can be significant for seismic hazard assessment. These findings support the development of orientation-dependent ground motion models and emphasize the importance of accurately representing azimuthal dependence and variability in hazard analysis and seismic design, especially in regions dominated by strike-slip faulting, such as California.

Introduction

Earthquake ground motions are typically recorded in two orthogonal horizontal components and one vertical component. Their intensity is usually captured by simplified parameters referred to as intensity measures (IMs). In earthquake engineering, the most commonly used IM is the 5%-damped response spectral ordinate, representing the peak response of a linear-elastic single-degree-of-freedom oscillator at a specified natural period. Numerous investigations have shown that horizontal ground-motion amplitudes vary significantly with changes in azimuth, a phenomenon often referred to as directionality (Hong and Goda, 2007; Shahi and Baker, 2014; Poulos and Miranda, 2022b). For instance, while studying baseline corrections of digital recordings, Boore et al. (2002) reported large differences in spectral ordinates between the two recorded horizontal components; similar findings were noted by Boore and Akkar (2003). Despite the widespread acknowledgment of directionality, current ground-motion models (GMMs) generally ignore it. Most available GMMs predict a single scalar IM, effectively omitting the dependence of amplitude on orientation. This has motivated work on identifying scalar IMs that best capture ground-motion amplitude and quantifying the relations between the scalars (Abrahamson and Silva, 1997; Beyer and Bommer, 2006; Boore, 2010; Boore et al., 2006; Boore and Kishida, 2016). Design provisions in many countries similarly neglect directionality or treat it indirectly. In the United States, for example, directionality has been addressed by requiring design based on the maximum horizontal intensity

(RotD100), which can be approximated by applying a period-dependent scale factor to the median over all orientations (RotD50) predicted by GMMs. Nevertheless, this remains a scalar approach and does not capture or take into account the full azimuthal variation of amplitude.

A key obstacle to developing orientation-dependent GMMs may have been that the azimuth associated with peak intensity is thought to be random beyond the near-fault region. Somerville et al. (1997) observed that response-spectrum values at periods greater than about 0.6 s tend to be larger in the strike-normal direction compared to those in the strike-parallel direction, suggesting a preferred orientation aligned with strike-normal. Subsequent studies found an increased likelihood that the orientation of maximum spectral response is close to strike-normal, but only at rupture distances less than about 5 km (Huang et al., 2009; NEHRP Consultants Joint Venture, 2011; Shahi and Baker, 2014). The prevailing conclusion from these works is that the azimuth of maximum spectral response relative to fault strike is effectively random and can be modeled as uniformly distributed for distances greater than 5 km. Accordingly, when conducting response history analyses, current U.S. seismic design standards use intensities and apply ground motions to structural models assuming that the orientation of peak intensity is random at larger source-to-site distances (ASCE, American Society of Civil Engineers, 2016, 2022).

Poulos and Miranda (2023) revisited this issue by considering the orientation of maximum spectral response relative to the epicentral transverse direction, i.e., the axis perpendicular to the line from the recording station to the epicenter. Unlike the strike-normal orientation, which is fixed for all stations for a given event, the epicentral transverse orientation varies with station location. Analyzing 2226 reverse-faulting and 1966 strike-slip records from earthquakes with moment magnitude greater than five from the NGA-West2 database, they showed that the preferred orientation of maximum spectral response depends on faulting style. For reverse-faulting events, the maximum response did not exhibit a consistent preferred azimuth; in contrast, for strike-slip earthquakes, maximum response spectral ordinates tended to occur close to the epicentral transverse direction, with this tendency becoming stronger as oscillator period increased. This finding indicates that the orientation of maximum spectral response is not uniformly distributed with respect to the epicentral transverse axis. A practical implication is that, for strike-slip events, the azimuth of maximum intensity can be inferred from the station's position relative to the epicenter which could lead to more accurate estimations of ground motion intensities.

These insights from Poulos and Miranda (2023) on directionality offer a practical foundation for estimating ground-motion amplitudes based on azimuth and, ultimately, for developing orientation-dependent ground-motion models. Specifically, if the azimuth of the RotD100 direction can be predicted relatively well for a site–event pair, the relatively stable pattern of spectral amplitudes referenced to that direction allows for more accurate prediction of intensities at all other orientations. Building on this idea, this paper summarizes our previous and ongoing efforts to understand directionality in strike-slip earthquakes, aiming to identify the factors that primarily control the orientation of maximum intensity and to quantify the amplitude of response spectral ordinates across all non-redundant orientations. The long-term goal is to develop orientation-dependent models that can be used in probabilistic seismic hazard analyses, improving upon current RotD50-based models. The initial focus on strike-slip sources is justified because they dominate seismic hazard in California and other regions around the world; for example, approximately 77% of California events with magnitude greater than 5 are strike-slip, so enhanced predictions of RotD100 orientation and azimuth-specific intensities for these earthquakes could significantly improve seismic hazard mapping in California. Therefore, in this short paper, we summarize our efforts to aggregate a new ground motion database of strike-slip records that includes recent events, briefly highlight new observational evidence of directionality from recent strike-slip recordings, and assess whether existing physics-based simulations of California strike-slip rupture reproduce these directional patterns, providing a comprehensive validation against empirical data. Lastly, we address the added aleatory variability caused by azimuthal dependence, which has been largely overlooked since the transition to orientation-independent IMs like RotD50, by developing improved methods to measure the component-to-component variance of spectral intensity with horizontal orientation.

Directionality in recent earthquakes

Poulos and Miranda (2023) based their analysis on the NGA-West2 ground-motion database. As part of our continuing efforts, we are augmenting this dataset with additional, well-instrumented recent (occurring after 2013) strike-slip events from California and other regions around the world. These new records provide an opportunity to independently assess the observations reported by Poulos and Miranda, and to develop improved ground motion models accounting for directionality. Some additional earthquakes we have identified and included in a database are the 2014 M_w 6.0 South Napa, 2016 M_w 5.2, Borrego Springs, 2019 M_w 7.1 Ridgecrest, 2019 M_w 6.4 Ridgecrest, 2020 M_w 6.5 Monte Cristo Range, 2021 M_w 5.3 Calipatria, 2022 M_w 6.4 Ferndale earthquakes, and 2024 M_w 7.0 Cape Mendocino earthquake.

To build the expanded dataset, we applied a series of screening steps. First, because studying directionality requires knowledge of both horizontal channels and their orientations, we retained only stations with two orthogonal horizontal recordings for which the component azimuths are documented. Second, we required that the ground motion records exhibit a peak ground velocity (PGV) of at least 0.1 cm/s; this threshold ensures adequate signal-to-noise over a wide period range, with particular benefits at longer periods. Third, for records meeting these criteria, linear oscillator responses were computed only up to the maximum usable period, taken as 1 divided by 1.25 times the low-pass corner frequency, consistent with the approach of Abrahamson and Silva (1997). This latter constraint helps ensure that long-period responses are not affected by the processing of the records. Finally, we performed a visual quality check and removed traces with recording problems, such as premature termination or delayed trigger.

As an example of results from the newly aggregated dataset, Figure 1 shows the spatial distribution of the orientation of maximum response spectral ordinates (i.e., intensity) for the 2024 M_w 7.0 Cape Mendocino earthquake. Following Boore (2010), the azimuth-specific spectral response at a site is obtained by first computing the relative displacement time histories of a 5%-damped SDOF oscillator for the two as-recorded horizontal components, then combining the two displacement histories into a single waveform associated with a specific azimuth within the plane (i.e., a projection), and rotating/repeating the process for different azimuths. The absolute peak of the rotated time series gives the spectral ordinate for that azimuth. The envelope over all non-redundant azimuths (0–180°) defines RotD100, and the corresponding azimuth is the direction of maximum response. In Figure 1, short black lines indicate the RotD100 direction at each station for 5 s and 10 s oscillators. Following Poulos and Miranda (2023), we denote by α the signed angular distance between the direction of maximum response and the epicentral transverse direction (i.e., the orientation perpendicular to the line from the station to the epicenter), with α ranging from −90° to +90°. The sign of α indicates whether RotD100 orientation is clockwise or counterclockwise with respect to the transverse orientation. In this study, we use |α|, which does not differentiate between clockwise or counterclockwise. In Figure 1, the colored circles indicate |α| for oscillators at different sites, with blue corresponding to small |α| (RotD100 near the transverse), and red indicating large |α| (RotD100 nearing the radial, i.e., along the station–epicenter line).

Figure 1 brings to light several key observations. First, as noted in other studies (Girmay, Poulos, et al., 2024; Poulos and Miranda, 2023), stations located near one another tend to exhibit similar RotD100 orientations (i.e., short black lines of adjacent stations tend to be similar). Second, numerous recording stations for this earthquake tend to have RotD100 orientations that occur close to the transverse orientation (i.e., blue colored circles, and black lines forming a circular pattern around the epicenter). However, it is also apparent that there appears to be a systematic deviation of RotD100 orientation from the transverse near the San Francisco Bay area (i.e., many red colored circles). This observation is contrary to what would be expected from the findings of Poulos and Miranda (2023) and others, who have observed that RotD100 orientation tends to occur close to the transverse at all locations around the epicenter. Evidently, Figure 1 suggests that there are clear azimuthal dependencies of RotD100 orientations within the horizontal plane (i.e., there might be systematic deviation from the transverse in specific source-to-site azimuths). Therefore, the newly aggregated database, which includes more data points and thus reduced azimuthal gaps in source-to-site paths, is currently being used to further analyze this azimuthal effect. Ultimately, the results of this study will be used to develop new orientation-dependent ground motion models that can be used to obtained improved seismic hazard curves at sites in California and other regions where hazard is dominated by strike-slip earthquakes.

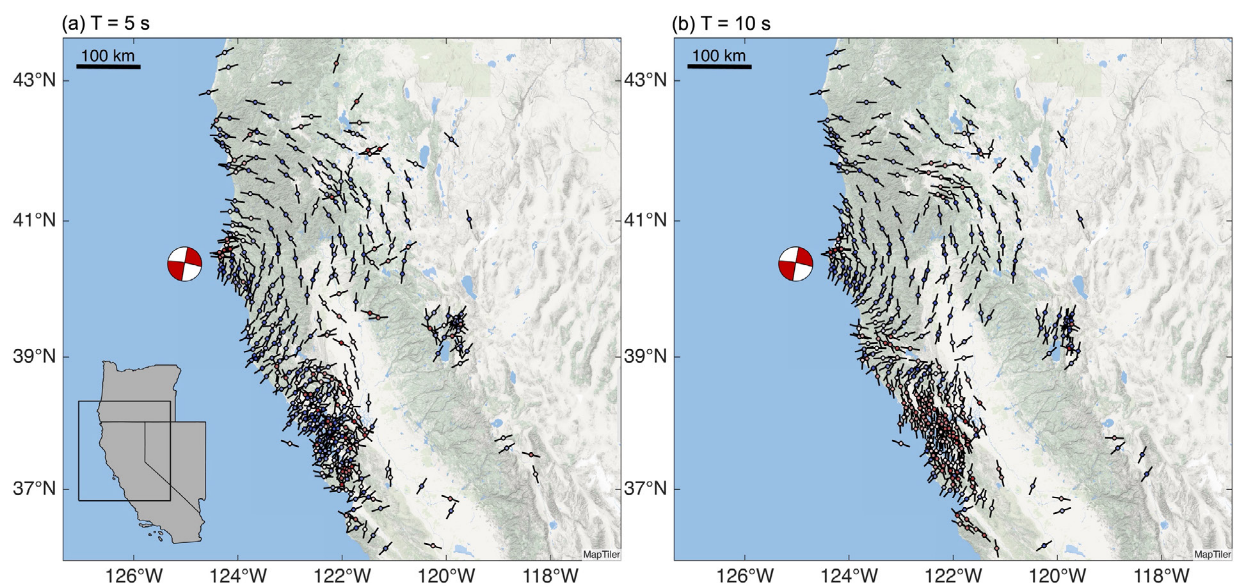

Figure 1: Orientation of maximum intensity of 5%-damped linear elastic oscillators subjected to ground motions from the 2024 M_w 7.0 Cape Mendocino earthquake. Short black lines at each station indicate the orientation of maximum response, and the color inside each circle indicates their angular distance from the transverse orientation.

Directionality in physics-based ground motion simulations of strike-slip earthquakes

Over recent decades, improvements in wave modeling and high-performance computing have enabled sophisticated physics-based simulations of earthquake ground motions (e.g., Graves and Pitarka, 2010; Mai et al., 2010). U.S. design provisions (ASCE, American Society of Civil Engineers, 2022) allow such simulations to serve as input for nonlinear response-history analyses when suitable recordings are unavailable. This is particularly advantageous for near-source, large-magnitude events, where empirical datasets remain sparse. However, engineering use is warranted only if simulations can reproduce key features of recorded motions, and a substantial body of work over the past decade has focused on validation for this purpose (e.g., Bijelić et al., 2018; Burks et al., 2015; Burks and Baker, 2014; Fayaz et al., 2020; Galasso et al., 2020; Teng and Baker, 2019). Despite extensive validation efforts, directionality has been comparatively underexplored in the context of simulations. Most studies that considered validation of directionality in simulations (e.g., Burks et al., 2015; Burks and Baker, 2014; Galasso et al., 2020; Teng and Baker, 2019) mostly only quantify the level of polarization using the RotD100/RotD50 ratio and have not evaluate other aspects of ground motion directionality. This leaves a gap concerning how spectral intensity varies with changes in orientation and the spatial distribution of the orientation of peak response.

Motivated by recent findings for strike-slip earthquakes by Poulos and Miranda (2023) and others (e.g., Girmay, Miranda, et al., 2024; Girmay, Poulos, et al., 2024), we investigate these aspects in physics-based simulations. A key premise of this work is that S waves from an ideal double-couple in a homogeneous medium are polarized transverse to the propagation direction. Testing whether physics-based simulations manifest similar behavior, particularly the alignment of the maximum response with the epicentral transverse orientation, is therefore important. To achieve this objective, we used CyberShake Study 15.12 (Graves et al., 2011) to evaluate directionality in simulated strike-slip events. In Girmay et al. (2025), we assess whether the hybrid broadband simulations capture directionality observed in recordings by analyzing the orientation of maximum spectral response and its spatial pattern for 5%-damped linear-elastic oscillators. We further examine how this preferred azimuth of maximum spectral response depends on rupture characteristics (e.g., rupture length, nucleation location, and propagation direction) and oscillator period, and we quantify in-plane polarization at each period by computing spectral accelerations across all nonredundant horizontal orientations.

This study used ground motions simulated at 334 stations from five rupture variations across two strike-slip scenarios on the Elsinore fault zone, totaling 1,670 records. The simulated scenarios correspond to M_w 6.95 and M_w 7.45 events. The smaller-magnitude case involves rupture of the Whittier and Glen Ivy segments (W + GI), while the larger case ruptures the Glen Ivy, Temecula, Julian, and Coyote Mountain segments (GI + T + J + CM). To examine the influence of the point of nucleation within the rupture (hypocenter location) and rupture propagation direction on the orientation of peak spectral response, rupture variations were selected to initiate at distinct hypocenter locations. For the W + GI scenario, hypocenters were placed at the southern end (south-to-north, S–N rupture), the northern end (north-to-south, N–S rupture), and near the center (approximately bilateral rupture). For the GI + T + J + CM scenario, hypocenters at the southern and northern ends of the rupture were considered. For each rupture realization and station, velocity seismograms were retrieved and numerically differentiated to obtain acceleration time series, which were then used to compute relative displacement responses of 5%-damped linear-elastic single-degree-of-freedom oscillators. To characterize the orientation of maximum spectral response, the angular distance between the RotD100 orientation and the epicentral transverse orientation (i.e., |α|) was computed, and its statistics were analyzed.

For a given oscillator period, should the orientation of maximum spectral response be equally likely to occur in any orientation with respect to the epicentral transverse orientation (i.e., should it be random with respect to the transverse), then the mean |α| over all stations for a given event would be equal to 45°. Thus, mean |α| values less than 45° indicate RotD100 orientations that are systematically closer to the transverse orientation, while mean |α| values larger than 45° indicate RotD100 orientations that are systematically closer to the radial orientation. Figure 2 indicates that the orientation of maximum spectral response for 5%-damped single-degree-of-freedom oscillators when subjected to physics-based simulations of strike-slip ruptures consistently occurs near the epicentral transverse orientation (i.e., mean |α| below 45°), consistent with recent observations from recorded strike-slip events. As the oscillator period increases, the orientation of maximum spectral response gets even closer to the transverse orientation for all rupture variations, following the trends of recorded ground motions from the NGA-West2 database.

Similarly, Figure 3 shows that orientation-specific spectral accelerations, when normalized by the median over all azimuths for each simulated ground motion and evaluated as a function of angular separation from the transverse orientation, generally display patterns comparable to those in NGA-West2 recordings. At longer periods, where wave scattering effects are less pronounced, the simulations show a mean variation of intensity as a function of angular distance from the transverse that closely aligns with that observed in recorded data. At shorter periods, where the hybrid broadband simulations use simplified scattering effects and semi-stochastic methods, the simulated ground motions result in a stronger level of response polarization when compared to recorded ground motions. This indicates that the hybrid approach does not fully capture scattering effects, particularly near the surface where the CyberShake Study 15.12 crustal model does not include shear-wave velocities below 500 m/s.

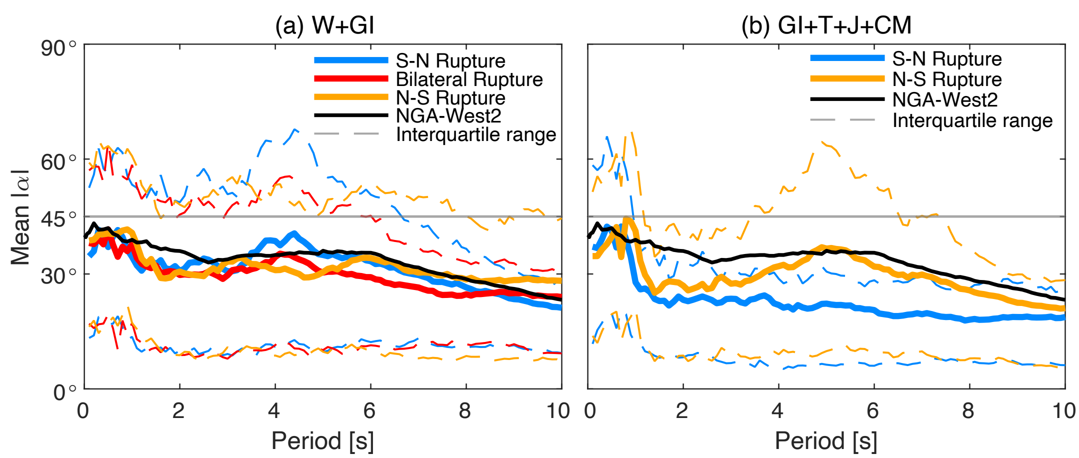

Figure 2: Influence of oscillator period on the mean angular distance between the orientation of maximum spectral response and the transverse orientation (i.e., mean $|\alpha|$) for different rupture variations on the Elsinore faults (a) W+GI segments, and (b) GI + T + J + CM segments. The dashed lines indicate interquartile ranges, and solid lines show the mean $|\alpha|$ for each rupture variation. The solid black curve shows the mean $|\alpha|$ for the NGA-West2 database. This figure is from Girmay et al. (2025).

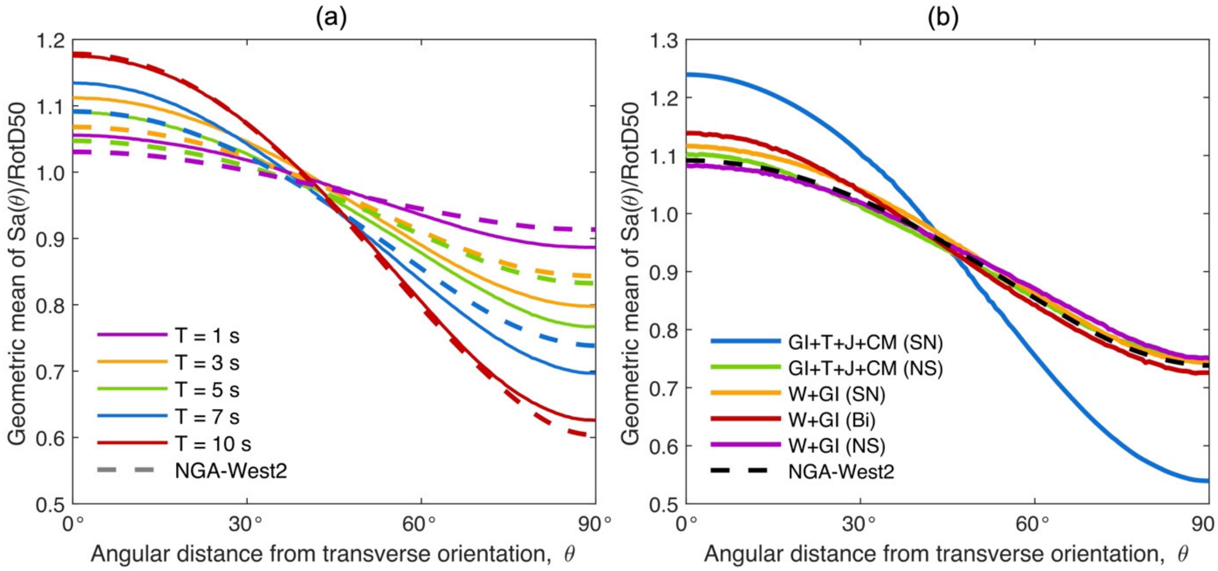

Figure 3: Influence of the angular distance from the transverse orientation on the geometric mean ratio of the response at a given angle from the transverse orientation and RotD50 intensity. In panel (a), the solid lines show the results when all the simulated ground motions used in the study are aggregated at different periods, while the dashed lines indicate the results for recorded ground motions from strike-slip earthquakes in the NGA-West2 database. In panel (b), the solid lines indicate the results for a 7 s oscillator subjected to simulated ground motions from different rupture variations, and the dashed line shows the result for strike-slip records from the NGA-West2 database. This figure is from Girmay et al. (2025).

Overall, these results indicate that physics-based ground motions for strike-slip earthquakes, despite resulting in a level of response polarization at short periods that is larger than that expected, capture relatively well most other directionality features present in recorded ground motions. This supports the use of simulated motions in appropriate engineering applications, especially for structures with fundamental periods exceeding about 1 s, where directionality effects are more pronounced. For more detailed information on directionality in physics-based ground motion simulations, the reader is referred to Girmay et al. (2025).

Component-to-component variability of spectral ordinates in strike-slip earthquakes

Structural engineers are primarily concerned with lateral deformation demands and, in particular, with peak story drift demands on the horizontal principal axes of the structure (e.g., longitudinal and transverse axes of a building). This is because structural elements such as beams, structural walls, and braces are typically aligned with these principal axes. Furthermore, many types of drift-sensitive nonstructural components, such as curtain walls, precast facade elements, and interior partitions, are also aligned with these axes. Therefore, compliance with the maximum drift limits in a certain story involves checking the maximum drifts regardless of whether this happens in the longitudinal or transverse directions. The same is true for many other structures such as bridges, dams, levies and other types of embankments or channels and ducts, where there is a primary emphasis on the maximum deformations occurring in the transverse and longitudinal axes of these structures. Therefore, estimation of intensity measures such as RotD50, which only provide information of the median intensity across orientations, is insufficient for engineering purposes, where there is an interest in estimating the probability of exceedance of ground motion intensities in specific orientation such as the principal axes of a structure. For example, if a site were to experience the RotD50 expected by a ground motion model (GMM), the probability that one of two orthogonal axes experiences a higher ground motion intensity is very high. In a recent study, Poulos and Miranda (2022a) showed that the probability of exceeding the RotD50 intensity in one of two orthogonal horizontal axes varies from 92% for short period structures to as high as 98% (almost certainty) for long period structures. Furthermore, the variability in RotD50 intensities does not account for component-to-component variability and therefore also underestimates the variability of response spectral ordinates at specific orientations that are of interest to engineers.

Ground motion models typically estimate earthquake ground motion intensity using scalar measures such as the geometric mean of spectral ordinates from two recorded horizontal components (GM_{xy}) or the median spectral ordinate across all orientations (RotD50). While several older GMMs primarily adopted GM_{xy}, modern GMMs largely prefer RotD50 due to its independence of the orientation of the horizontal sensors. Accurate quantification and modeling of variability around these scalar measures are essential for incorporating and propagating uncertainty in Probabilistic Seismic Hazard Analyses (PSHA). This variability significantly impacts seismic response estimates and the evaluation of seismic risk, especially at lower annual frequencies common in engineering designs.

In GMMs, the residuals' natural logarithm is assumed to be normally distributed, with the standard deviation (σ) representing the total aleatory uncertainty. This includes within-event (ϕ) and between-events (τ) standard deviations, combined as $\sqrt{\phi^2 + \tau^2}$. However, horizontal spectral ordinates also vary significantly within a site with changes in orientation, introducing an additional uncertainty termed component-to-component variability (σ_{c2c}^2), which is required to obtain the uncertainty of the arbitrary or random horizontal component. This variability should also be included in PSHA, particularly for estimating ground motion intensity in arbitrary or specific orientations relevant to structural responses. The total variability of the ground motion intensity at specific orientations (often also referred to as the arbitrary component) can hence be calculated as $\sqrt{\phi^2 + \tau^2 + \sigma_{c2c}^2}$.

Component-to-component variability has traditionally been computed as the arithmetic mean of the squares of the component-to-component residuals for a database of ground motions (Boore, 2005; Boore et al., 1997). Mathematically, it is computed as

$$\sigma_{c2c}^2 = \frac{1}{N}\sum_{j=1}^{N}\left(\frac{\ln Y_{x,j} - \ln Y_{y,j}}{2}\right)^2 \quad [1]$$

where N is the number of records, and $Y_{x,j}$ and $Y_{y,j}$ are the pseudo-acceleration response spectral ordinates in the as recorded orientations of the jth record. This traditional definition can also be interpreted as the ratio in ground motion intensity between the two as recorded horizontal orientations. As shown in Eq. [1], it is a function of the difference of the natural logarithms of ground motion intensity in the two as-recorded horizontal orientations, which could be notably different depending on the orientation of the sensors. To clearly illustrate this issue, Figure 4

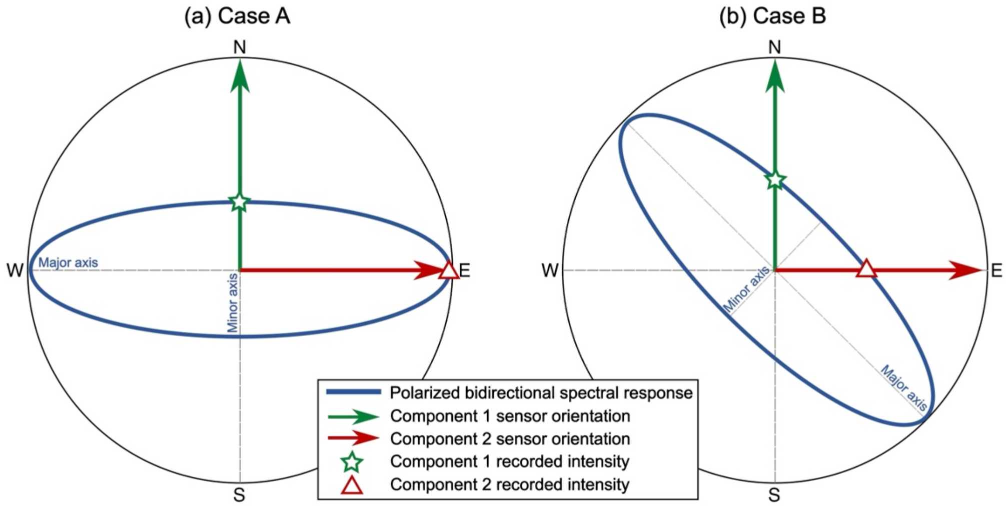

Figure 4: An illustration of an idealized polarized horizontal response of an oscillator. The colored arrows indicate sensor orientations, and the markers represent the spectral response in the sensor orientations when (a) the sensors are aligned with the major and minor response axes, and (b) when the sensors are orientated at 45° from the major response axis. This figure is taken from Girmay and Miranda (2025).

shows the two extreme cases that could occur with polarized ground motions. In Case A, the major response axis aligns with one of the recorded components, resulting in a large component-to-component variability. In contrast, in Case B, the major response axis for the same motion occurs at 45° from the sensor orientations, which causes the intensity in the as-recorded components to be approximately equal, ultimately resulting in a much smaller or even null component-to-component variability. Therefore, this traditional method, like GM_{xy}, is influenced by sensor orientation, which may lead to systematic overestimations or underestimations across numerous stations depending on the location of the epicenter relative to the stations and the sensor orientations at those stations. Since horizontal sensors in free field stations are typically oriented in NS and EW directions, then, for specific earthquakes, σ_{c2c} could be strongly biased to either overestimate or underestimate the component-to-component variability in the event.

Recent studies and GMM emphasize the importance of using measures of intensity that are unaffected by sensor orientation, leading to the widespread adoption of RotD50 in GMMs and seismic hazard analyses. However, most existing GMMs that use RotD50 do not provide estimates for component-to-component variability, and many of the associated papers often do not discuss this additional source of uncertainty. This is most likely because hazard modeling is performed using RotD50 and U.S seismic design standards warrant the use of RotD100 (maximum direction intensity), hence it may be believed that there is no need to use the arbitrary component or estimate its uncertainty. Despite misconceptions about its necessity in 3D structural analyses, incorporating component-to-component variability is crucial for accurate exceedance probability estimation in structures. This is because, fundamentally, structures do not "feel" RotD50 or RotD100 intensities in their principal axes, but instead they experience ground motion intensities that exhibit strong variations in amplitude with changes in orientation. Thus, the best representation of seismic demand on a structure's principal axes is the arbitrary component, and the probability of exceedance of certain limit states in the principal axes of structures should be based on the total variability accounting for the component-to-component variability. Failing to account for the component-to-component variability would result in an underestimation of the total variability of the spectral ordinates in the random principal axes orientation, which would artificially result in a lower rate of exceedance for a given spectral acceleration (i.e., leading to unconservative designs).

To address the gaps in current methods, as part of this project, we have studied improved ways of computing this component-to-component variability and have quantified it for various earthquakes. In Girmay and Miranda (2025) we propose new orientation-independent equations to quantify component-to-component variability, which can be used to obtain the total uncertainty of the arbitrary component from different measures of central tendency. For example, if a GMM is using the GM_{xy}, the component-to-component variability around GM_{xy} that is independent of the orientation of the sensors can be computed by first determining the spectral ordinates in all non-redundant rotation angles using a rotation angle increment of 1°, then averaging the component-to-component residual for all orientations as follows

$$\sigma_{c2c}^2 = \frac{1}{N}\sum_{j=1}^{N}\frac{1}{180}\sum_{i=1}^{180}\left(\ln Y_{i,j} - \frac{\ln Y_{x,j} + \ln Y_{y,j}}{2}\right)^2 \qquad [2]$$

where N is the number of records, $Y_{i,j}$ is the pseudo-acceleration response spectral ordinate corresponding to the ith component of the jth record, and $Y_{x,j}$ and $Y_{y,j}$ are the pseudo-acceleration response spectral ordinates in the recorded orientations of the jth record. Equation [2], henceforth referred to as Definition 2, is an improvement of the traditional definition (equation [1]) since the resulting component-to-component variability value does not depend on the orientation of the sensors (i.e., it would result in the same value for a given ground motion regardless of the direction in which the orthogonal horizontal sensors sample the ground motion).

Similarly, if a GMM uses the RotD50 intensity, as most current models do, the component-to-component variability can be obtained from the RotD50 intensity as follows

$$\sigma_{c2c}^2 = \frac{1}{N}\sum_{j=1}^{N}\frac{1}{180}\sum_{i=1}^{180}\left(\ln Y_{i,j} - \ln Y_{RotD50,j}\right)^2 \qquad [3]$$

where $Y_{RotD50,j}$ is the RotD50 pseudo-acceleration response spectral ordinate for the jth record. Equation [3], will be referred to herein as Definition 3 going forward.

To understand the differences between the definitions of component-to-component variability introduced above, equations [1] to [3] can be computed for a database of ground motion records and compared. While the equations above can be applied to records from any type of faulting mechanism, here we demonstrate the differences between them using strike-slip records from the NGA-West2 database, plus the additional California earthquakes identified earlier in this paper (see section 2 of this paper), for a total of 4,331 records. Using strike-slip earthquakes is interesting because recent studies have reported that they result in systematically polarized responses of oscillators even at far distances from the rupture. This leads to extensive geographic regions where strongly polarized motions may occur, making it important to accurately quantify and account for the component-to-component variability.

To compare and understand the changes in component-to-component variability across different earthquakes, Figure 5 illustrates the effect of oscillator period on component-to-component variability using Definitions 1–3, based on data from 79 strike-slip earthquakes. Gray lines represent individual earthquake data, while the solid black line depicts the median of the variability computed from 4,331 records across all events. As shown for all three definitions, there is a tendency for this component-to-component variability to increase with increasing periods. This is the result of the increase in polarization of the ground motions with increasing periods. Another way to state this is that in shorter periods, the level of polarization in ground motions is reduced due to greater scattering in waves with shorter wavelengths. The variability of the gray lines around the black line reveals that there are significant earthquake-to-earthquake differences in component-to-component variability for all three definitions. However, Definition 1 shows a notably higher earthquake-to-earthquake variability compared to that of Definitions 2 and 3, which exhibit similar levels of variability between them. This is because in Definition 1, the variation of intensity depends on sensor orientation, and fundamentally (as shown in Eq. [1]), only measures the difference in ground motion intensity in the two as-recorded orientations, neglecting the variation of ground motion intensity at orientations where the motion was not recorded. In reality, and as illustrated in Figure 4, the real component-to-component variability may be larger or smaller than that estimated with Definition 1, depending on how the horizontal sensors are oriented relative to the orientation of the maximum intensity. Meanwhile, definitions 2 and 3 account for the variation in intensity at all non-redundant orientations and therefore provide better characterizations of this variability. By removing the dependence on the orientation of the horizontal sensors, Definitions 2 and 3 result in reduced variability around the black line and in higher median variability for longer periods. Additionally, the tendency for stations within specific regions to share similar sensor orientations, combined with spatial trends in polarization that are influenced by the epicenter's position relative to the stations (Girmay, Poulos, et al., 2024; Poulos and Miranda, 2023), results in an inherent bias of the component-to-component variability for Definition 1.

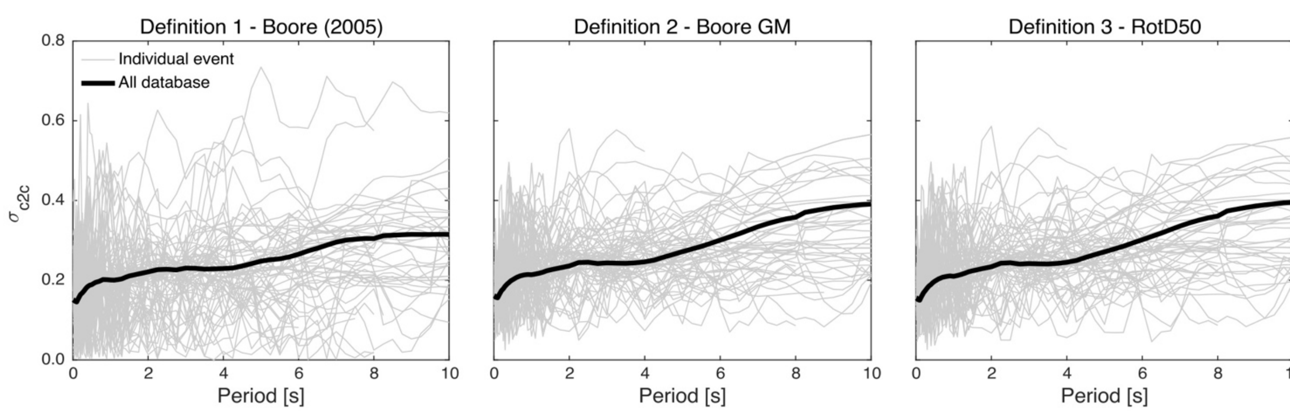

Figure 5: Influence of oscillator period on component-to-component variability for 79 different strike-slip earthquakes when using definitions 1, 2 and 3. This figure is taken after Girmay and Miranda (2025).

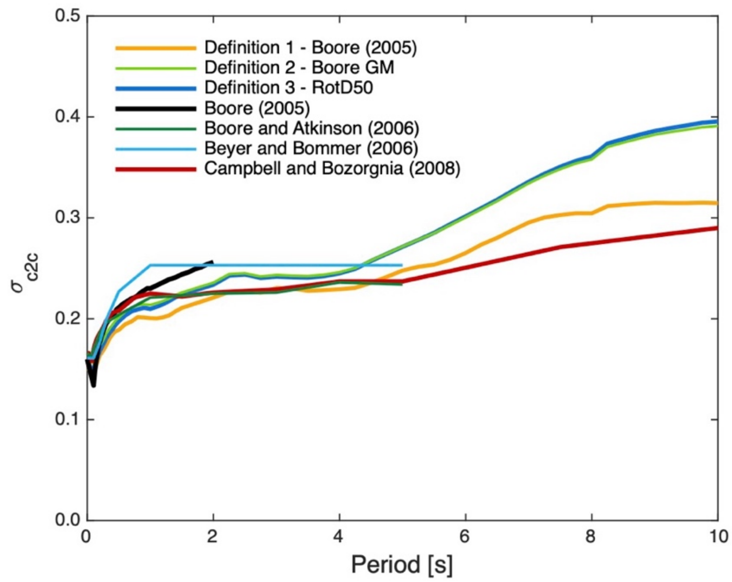

Figure 6: Component-to-component variability for Definitions 1, 2, and 3 computed for 4,331 records. Also shown for comparison are values for component-to-component variability computed by others. Values for Beyer and Bommer (2006) and Boore and Atkinson (2006) are as reported in Table 1 of Watson-Lamprey and Boore (2007). This figure is taken after Girmay and Miranda (2025).

Figure 6 provides a comparison of component-to-component variabilities for Definitions 1, 2, and 3 as functions of oscillator period when using 4,331 records. It also includes previously reported variabilities for Definition 1 (Boore, 2005; Campbell and Bozorgnia, 2008; Watson-Lamprey and Boore, 2007), with values for Boore and Atkinson (2006) and Beyer and Bommer (2006) extracted from Table 1 in Watson-Lamprey and Boore (2007). Evidently, all definitions show increasing component-to-component variability with increasing oscillator period, which can be attributed to the increase in the level of directionality and polarization with oscillator period. Although Definition 1, which depends on sensor orientation, exhibits a similar level of variability to Definition 2 for periods shorter than 5 s, it yields lower variabilities than Definition 2 for longer periods where polarization is significant. Definition 3 generally produces component-to-component variabilities similar to those of Definition 2, but shows a marginally higher variability at long periods. When comparing these results with prior studies focusing on Definition 1, it appears that this study's dataset leads to lower variability for short periods yet significantly higher variability for long periods. This disparity likely arises from the smaller datasets and mixed faulting mechanisms used by others, suggesting that component-to-component variability may be influenced by style of faulting. Strike-slip earthquakes may exhibit lower component-to-component variability in short periods but higher variability in long periods.

As previously hinted, spatial trends in polarization, combined with alignment of sensor orientations across stations within specific geographic regions, can result in significant differences in component-to-component variability when using Definitions 1 and 2. To demonstrate this issue, short black lines are used in Figure 7a to indicate the orientation of maximum response for 10 s oscillators at each station in the LA metropolitan region that recorded the 2016 M_w 5.2 Borrego Springs earthquake. At each station, the short red lines show horizontal sensor orientations. As is the case with most free-field stations, the orientations of most sensors that recorded this earthquake tend to be in the north-south and east-west directions.

Consistent with the observations of others for different strike-slip earthquakes (e.g., Girmay, Poulos, et al., 2024; Poulos and Miranda, 2023), the orientation of maximum spectral response for neighboring stations tends to be similar. For this particular earthquake and in this geographic region, the orientation of maximum response at most recording stations is approximately 45° from the orientation of the horizontal sensors. This alignment results in response spectral ordinates in the recorded orientations being similar to each other, corresponding to Case B in Figure 4. Consequently, within this geographic region, using Definition 1 underestimates the component-to-component variability across stations compared to Definition 2, which is not influenced by the orientation of the horizontal sensors. This is clearly apparent in Figure 7b, where the curve for Definition 1 is significantly lower than that for Definition 2 for most periods but particularly for periods longer than 3 s.

As explained earlier in this paper, estimating the probability of exceedance for limit states in engineered structures necessitates considering component-to-component variability because the demand along the principal axes of structures is affected by this additional source of variability. Therefore, seismic demands at these axes are better represented by the arbitrary component, whether conducting two-dimensional or three-dimensional analyses. The significance of component-to-component variability in earthquake engineering can become substantial if it reaches a level comparable to variabilities currently considered. Therefore, evaluating the impact (or level of significance) of component-to-component variability requires comparing it directly with the intra-event and inter-event variabilities commonly included in modern ground motion models (GMMs) and PSHA.

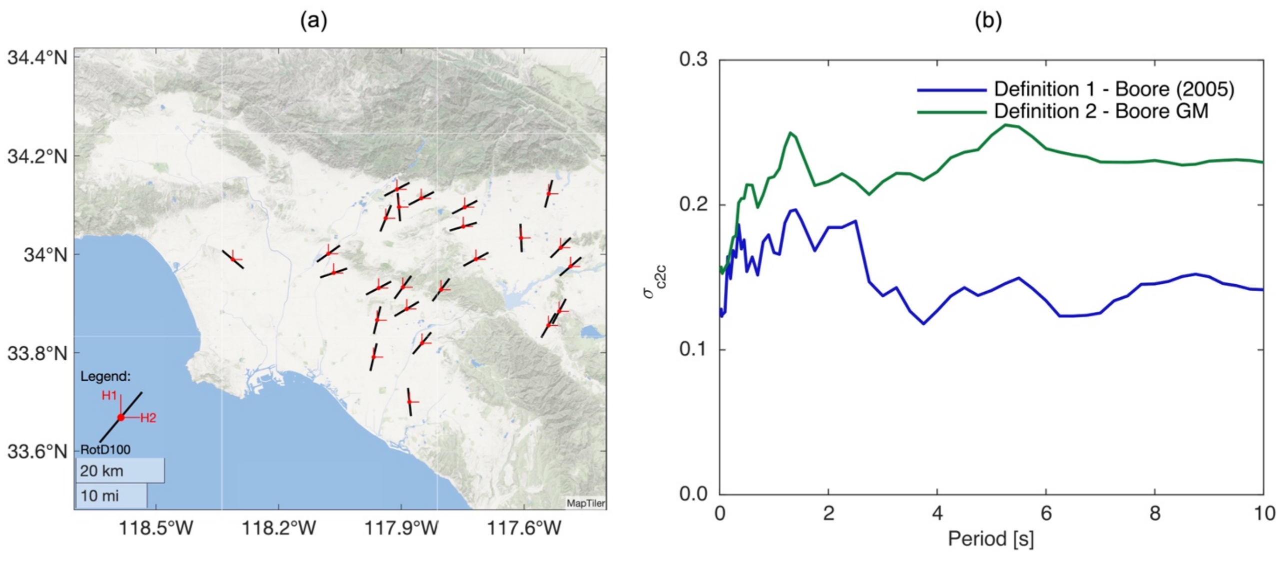

Figure 7: (a) Horizontal sensor orientations in the Los Angeles metropolitan region (shown by the red lines) at each seismic station that recorded the 2016 M_w 5.2 Borrego Springs earthquake, and the corresponding orientation of maximum response for 10 s oscillators (shown by the short black lines); (b) Influence of oscillator period on the component-to-component variability within the Los Angeles metropolitan region for the 2016 M_w 5.2 Borrego Springs earthquake. This figure is taken after Girmay and Miranda (2025).

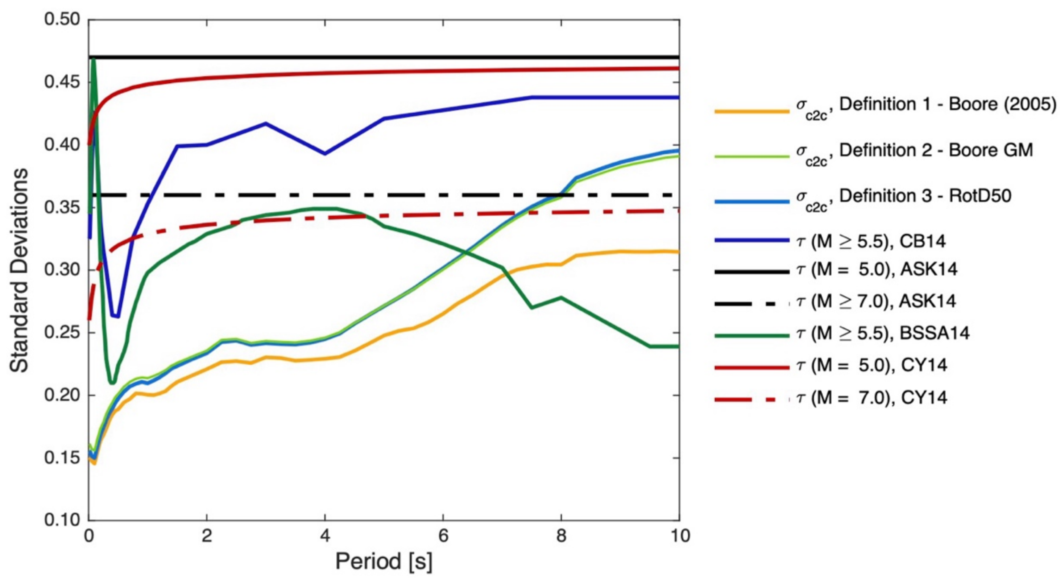

Figure 8: Component-to-component variability for Definitions 1, 2, and 3, compared to between-event variabilities from NGA-West2 GMMs.

Figure 8 illustrates the comparison of component-to-component variability for Definitions 1-3, computed using 4,331 strike-slip records, against magnitude-dependent between-event (also referred to as earthquake-to-earthquake) standard deviation of residuals from four NGA-West2 GMMs. These ground motion models provide estimates for the RotD50 intensity. Their between-event standard deviations are hence more directly comparable to Definition 3. From this figure, it is evident that component-to-component variability is relatively small compared to between-event standard deviations for shorter periods. However, in the middle period range and for larger magnitude events, this difference diminishes. At long periods, component-to-component variability matches or exceeds the between-event standard deviations for large-magnitude earthquakes, particularly surpassing BSSA14's between-event variability. This indicates that component-to-component variability could substantially impact seismic hazard estimation at a site. As we move towards non-ergodic GMMs, which tend to reduce between- and within-event variabilities compared to traditional ergodic models, the significance of component-to-component variability may increase, as it can get as large as the inter-event variability for medium to long periods.

Summary and conclusions

This paper summarizes ongoing efforts to study directionality of ground motions in strike-slip earthquakes through recent observational data, improved ground motion databases, and advanced physics-based simulations. It was found that ground motion amplitudes exhibit systematic directional patterns, especially for strike-slip earthquakes in California and other similar tectonic environments. Specifically, the orientation of maximum horizontal spectral response, traditionally considered random beyond near-fault distances (e.g., at distances from the rupture longer than 5 km), frequently occurs at orientations close to the epicentral transverse direction, with a tendency to occur even closer to the transverse with increasing period. This trend occurs even at large distances from the source, such as distances of 200 km away. These findings indicate that the orientation of maximum orientation can be predicted from information of the earthquake epicenter, which is usually randomized in PSHA. So, it is possible to consider the orientation of maximum response by using orientation-dependent ground motion models. These models can provide improved estimates of ground motion intensity in future strike-slip earthquakes, which are important for California.

Ongoing efforts to aggregate a new, comprehensive database, including several recent well-instrumented earthquakes, allow for a more robust evaluation of directionality and polarization effects. Spatial analysis of data from recent earthquakes revealed a consistent alignment of the orientation of maximum spectral response among neighboring stations, although localized deviations highlight the complexity of azimuthal dependencies in ground motion. We are currently working on quantifying the additional azimuthal dependencies using the large database of ground motions. Additionally, comparison of physics-based ground motion simulations with recorded ground motions from strike-slip earthquakes demonstrated that modern modeling techniques can successfully reproduce the observed patterns of directionality, particularly at periods above one second, while also revealing certain limitations in capturing scattering effects at shorter periods.

Structures do not “feel” RotD50 or RotD100 intensities in their principal axes, but instead they experience ground motion intensities that exhibit strong variations in amplitude with changes in orientation. Structural engineers are primarily concerned with seismic demands on the horizontal principal axes of the structure (e.g., longitudinal and transverse axes of a building). This is because structural elements such as beams, structural walls, and braces are typically aligned to these principal axes. Furthermore, many types of drift-sensitive nonstructural components, such as curtain walls, precast facade elements, and interior partitions, are typically also aligned to the principal axes of buildings. Therefore, compliance with the maximum drift limits in a certain story involves checking the maximum drift ratios regardless of whether this happens in the longitudinal or in the transverse directions. The same is true for many other structures such as bridges, dams, levies, and other types of embankments or channels, ducts and other types of man-made structure to transport liquids where there is a primary emphasis on the maximum deformations occurring in the transverse and longitudinal axes of these structures or elements. Therefore, estimation of intensity measures such as RotD50, which only provide information of the median intensity across orientations, is insufficient for engineering purposes, where there is an interest in estimating the probability of exceedance of ground motion intensities in specific orientation such as the principal axes of a structure. Recent studies have shown that if a site were to experience the RotD50 expected by a ground motion model (GMM), the probability that one of two orthogonal axes experiences a higher ground motion intensity is as high as 92% for short period structures to as high as 98% (almost certainty) for long period structures. Furthermore, the variability in RotD50 intensities does not account for component-to-component variability and therefore also underestimates the variability of response spectral ordinates at specific orientations that are of interest to engineers.

One important outcome of this work is the improved quantification of component-to-component variability. Traditional methods, which depend on sensor orientation, can misrepresent the true variability of the arbitrary component. The new, orientation-independent measures of component-to-component variability proposed in our research provide a more accurate characterization of the total aleatory variability of the arbitrary component, especially at longer periods where polarization is strong. Recognizing and correctly quantifying this variability is important, as its magnitude at long periods is comparable or can even exceed the between-event variability of response spectral ordinates, with direct implications for seismic hazard analysis and the probabilistic estimation of structural performance.

It is important to account for directionality and component-to-component variability in seismic hazard assessment and earthquake engineering. Incorporating the insights from the research discussed in this paper into ground motion models is pertinent for regions with significant strike-slip seismic risk, such as California. Ultimately, advancing the development of orientation-dependent ground motion modeling and precise variability quantification will lead to improved hazard assessments and engineering design, better safeguarding infrastructure and communities against earthquake risks.

Acknowledgments

Funding for this research was provided by the California Department of Conservation, California Geological Survey, Strong Motion Instrumentation Program Contract No. 1023-003. Partial funding for the doctoral studies of the second author was provided by the Shah Fellowship on Catastrophic Risk and the John A. Blume Fellowship from the Department of Civil Engineering at Stanford University.

References

Abrahamson NA and Silva WJ (1997) Empirical Response Spectral Attenuation Relations for Shallow Crustal Earthquakes. *Seismological Research Letters* 68(1): 94–127.

ASCE, American Society of Civil Engineers (ed.) (2016) *Minimum Design Loads and Associated Criteria for Buildings and Other Structures*. Reston, Virginia: American Society of Civil Engineers.

ASCE, American Society of Civil Engineers (ed.) (2022) *Minimum Design Loads and Associated Criteria for Buildings and Other Structures: ASCE/SEI 7-22*. Reston: American Society of Civil Engineers.

Beyer K and Bommer JJ (2006) Relationships between Median Values and between Aleatory Variabilities for Different Definitions of the Horizontal Component of Motion. *Bulletin of the Seismological Society of America* 96(4A): 1512–1522.

Bijelić N, Lin T and Deierlein GG (2018) Validation of the SCEC Broadband Platform simulations for tall building risk assessments considering spectral shape and duration of the ground motion. *Earthquake Engineering & Structural Dynamics* 47(11): 2233–2251.

Boore DM (2005) Erratum: Equations for Estimating Horizontal Response Spectra and Peak Acceleration from Western North American Earthquakes: A Summary of Recent Work. *Seismological Research Letters* 76(3): 368–369.

Boore DM (2010) Orientation-Independent, Nongeometric-Mean Measures of Seismic Intensity from Two Horizontal Components of Motion. *Bulletin of the Seismological Society of America* 100(4): 1830–1835.

Boore DM and Akkar S (2003) Effect of causal and acausal filters on elastic and inelastic response spectra. *Earthquake Engineering & Structural Dynamics* 32(11): 1729–1748.

Boore DM and Kishida T (2016) Relations between Some Horizontal-Component Ground-Motion Intensity Measures Used in Practice. *Bulletin of the Seismological Society of America* 107(1): 334–343.

Boore DM, Joyner WB and Fumal TE (1997) Equations for Estimating Horizontal Response Spectra and Peak Acceleration from Western North American Earthquakes: A Summary of Recent Work. *Seismological Research Letters* 68(1): 128–153.

Boore DM, Stephens CD and Joyner WB (2002) Comments on Baseline Correction of Digital Strong-Motion Data: Examples from the 1999 Hector Mine, California, Earthquake. *Bulletin of the Seismological Society of America* 92(4): 1543–1560.

Boore DM, Watson-Lamprey J and Abrahamson NA (2006) Orientation-Independent Measures of Ground Motion. *Bulletin of the Seismological Society of America* 96(4A): 1502–1511.

Burks LS and Baker JW (2014) Validation of Ground-Motion Simulations through Simple Proxies for the Response of Engineered Systems. *Bulletin of the Seismological Society of America* 104(4): 1930–1946.

Burks LS, Zimmerman RB and Baker JW (2015) Evaluation of Hybrid Broadband Ground Motion Simulations for Response History Analysis and Design. *Earthquake Spectra* 31(3). SAGE Publications Ltd STM: 1691–1710.

Campbell KW and Bozorgnia Y (2008) NGA Ground Motion Model for the Geometric Mean Horizontal Component of PGA, PGV, PGD and 5% Damped Linear Elastic Response Spectra for Periods Ranging from 0.01 to 10 s. *Earthquake Spectra* 24(1): 139–171.

Fayaz J, Azar S, Dabaghi M, et al. (2020) Methodology for Validation of Simulated Ground Motions for Seismic Response Assessment: Application to CyberShake Source-Based Ground Motions. *Bulletin of the Seismological Society of America* 111(1): 226–241.

Galasso C, Kaviani P, Tsioulou A, et al. (2020) Validation of Ground Motion Simulations for Historical Events using Skewed Bridges. *Journal of Earthquake Engineering* 24(10). Taylor & Francis: 1652–1674.

Girmay N and Miranda E (2025) Component-to-component variability of response spectral ordinates from strike slip earthquakes accounting for orientation of horizontal recorders. *Submitted to Earthquake Spectra for review and possible publication*.

Girmay N, Poulos A and Miranda E (2024) Directionality and polarization of response spectral ordinates in the 2023 Kahramanmaras, Türkiye earthquake doublet. *Earthquake Spectra* 40(1): 486–504.

Girmay N, Miranda E and Poulos A (2024) Orientation and intensity of maximum response spectral ordinates during the December 20, 2022 Mw 6.4 Ferndale, California earthquake. *Soil Dynamics and Earthquake Engineering* 176: 108323.

Girmay N, Poulos A and Miranda E (2025) Evaluation of directionality in physics-based ground motion simulations of strike-slip earthquakes. *Earthquake Spectra* 41(1): 436–456.

Graves R, Jordan TH, Callaghan S, et al. (2011) CyberShake: A Physics-Based Seismic Hazard Model for Southern California. *Pure and Applied Geophysics* 168(3): 367–381.

Graves RW and Pitarka A (2010) Broadband Ground-Motion Simulation Using a Hybrid Approach. *Bulletin of the Seismological Society of America* 100(5A): 2095–2123.

Hong HP and Goda K (2007) Orientation-Dependent Ground-Motion Measure for Seismic-Hazard Assessment. *Bulletin of the Seismological Society of America* 97(5): 1525–1538.

Huang Y-N, Whittaker AS and Luco N (2009) Orientation of Maximum Spectral Demand in the Near-Fault Region. *Earthquake Spectra* 25(3). SAGE Publications Ltd STM: 707–717.

Mai PM, Imperatori W and Olsen KB (2010) Hybrid Broadband Ground-Motion Simulations: Combining Long-Period Deterministic Synthetics with High-Frequency Multiple S-to-S Backscattering. *Bulletin of the Seismological Society of America* 100(5A): 2124–2142.

NEHRP Consultants Joint Venture (2011) *Selecting and Scaling Earthquake Ground Motions for Performing Response-History Analysis,*. NIST GCR 11-917-15, Technical Report. Available at: https://www.nehrp.gov/pdf/nistgcr11-917-15.pdf (accessed 3 August 2023).

Poulos, A., & Miranda, E. (2022a). Proposal of orientation-independent measure of intensity for *Earthquake Spectra 38*

Poulos A and Miranda E (2022b) Probabilistic characterization of the directionality of horizontal earthquake response spectra. *Earthquake Engineering & Structural Dynamics* 51(9): 2077–2090.

Poulos A and Miranda E (2023) Effect of Style of Faulting on the Orientation of Maximum Horizontal Earthquake Response Spectra. *Bulletin of the Seismological Society of America* 113(5): 2092–2105.

Shahi SK and Baker JW (2014) NGA-West2 Models for Ground Motion Directionality. *Earthquake Spectra* 30(3). SAGE Publications Ltd STM: 1285–1300.

Somerville PG, Smith NF, Graves RW, et al. (1997) Modification of Empirical Strong Ground Motion Attenuation Relations to Include the Amplitude and Duration Effects of Rupture Directivity. *Seismological Research Letters* 68(1): 199–222.

Teng G and Baker J (2019) Evaluation of SCEC CyberShake Ground Motions for Engineering Practice. *Earthquake Spectra* 35(3). SAGE Publications Ltd STM: 1311–1328.

Watson-Lamprey JA and Boore DM (2007) Beyond SaGMRotI: Conversion to SaArb, Sasn, and SaMaxRot. *Bulletin of the Seismological Society of America* 97(5): 1511–1524.